*Acta Physica Polonica B* **57**, 8-A1 (2026)

# HYPERON LONGITUDINAL POLARIZATION AND VECTOR MESON SPIN ALIGNMENT IN A THERMAL MODEL FOR HEAVY-ION COLLISIONS

Soham Banerjee [a], Samapan Bhadury [b]
Wojciech Florkowski [c], Amaresh Jaiswal [a]
Radoslaw Ryblewski [d]

[a]School of Physical Sciences
National Institute of Science Education and Research
An OCC of Homi Bhabha National Institute, Jatni, 752050, India
[b]Department of Physical Sciences
Indian Institute of Science Education and Research Berhampur
Laudigam-760003, District-Ganjam, Odisha, India
[c]Institute of Theoretical Physics, Jagiellonian University, 30-348 Kraków, Poland
[d]Institute of Nuclear Physics Polish Academy of Sciences, 31-342 Kraków, Poland

*Received 16 April 2026, accepted 20 April 2026,*
*published online 7 July 2026*

The concept of a common local spin equilibrium for both spin-1/2 and spin-1 particles is incorporated into a thermal model of particle production in heavy-ion collisions at the top RHIC energies. We show that an effective spin polarization tensor leading to a correct description of the longitudinal spin polarization of $\Lambda$ hyperons simultaneously yields a positive alignment of vector mesons ($\phi$ and $K^{*0}$) that grows monotonically with transverse momentum and centrality. Similar trends can be seen in the data, suggesting a possible common mechanism for longitudinal spin polarization and alignment. However, model calculations are insufficient to explain the data in a fully quantitative way. The correlation found between the magnitude of the $\Lambda$ longitudinal polarization and vector meson alignment suggests further more elaborate investigations of this issue.

DOI:10.5506/APhysPolB.57.8-A1

## 1. Introduction

The experimental investigations of spin polarization effects in relativistic heavy-ion collisions offer new possibilities for studying the properties of strongly interacting matter. These studies focus mainly on measurements of hyperon spin polarization [1–9] and vector meson spin alignment [10–12]; for recent reviews, see [13–15] and for various related theoretical developments, see [16–61].

For some time, the main difficulty in describing the $\Lambda$ polarization data was to reproduce the experimental results for the longitudinal component of the polarization vector (*i.e.*, the component along the beam direction) [62]. The proposed solutions to this problem include now adding the effects due to thermal shear [63–66] and/or a variation of the mass of the spin-polarized particle [64]. Yet another solution is to use the spin polarization tensor obtained from spin hydrodynamics [67, 68]. On the other hand, many theoretical frameworks yield a negative spin alignment of vector mesons [17, 19, 26, 40, 55], which is incompatible with the data, with the exception of the model presented in [26, 60, 69].

In this work, we use a recently proposed uniform description for the local equilibrium of spin-1/2 and spin-1 particles [70] to simultaneously address the two problems outlined above. To make our study as simple as possible, we use the framework of the thermal model used before to analyze the $\Lambda$ polarization at the top RHIC energies [71–74]. Since we consider high energies, the model is boost-invariant, however, it incorporates an anisotropic form of the transverse-flow responsible for the non-zero elliptic flow.

The conclusion of [74] is that the longitudinal spin polarization can be described by using a thermal vorticity, $\varpi_{\mu\nu} = -\frac{1}{2}\left(\partial_\mu \beta_\nu - \partial_\nu \beta_\mu\right)$ (where $\beta_\mu$ is the ratio of fluid four-velocity $u_\mu$ to temperature $T$) with neglected "electric"-like components. As found in our previous work [72], this procedure is consistent with a non-relativistic treatment where the polarization is solely determined by the spatial components of the rotation $\partial_i v_j - \partial_j v_i$ [75]. In this work, we additionally introduce a scale parameter $\lambda$ that multiplies the thermal vorticity, and is used to check the sensitivity of our results to the magnitude of the longitudinal polarization of $\Lambda$ hyperons.

With the form of the spin polarization tensor defined as the thermal vorticity (calculated directly in the thermal model) with neglected "electric"-like part and rescaled by a factor $\lambda$, we calculate the parameter $\rho_{00}$ of the spin density matrix of vector mesons as a function of transverse momentum and centrality. We also present the results for the $p_{\rm T}$-integrated values and their dependence on the direction of the quantization axis.

Our results establish a quantitative connection between the spin observables of the spin-1/2 and spin-1 hadrons that are in a common local spin equilibrium. We demonstrate that a non-trivial spin alignment arises in such a state without requiring the inclusion of dissipative phenomena — as the spin alignment is usually attributed to the spin fluctuations, it may appear also in the state of local equilibrium where only the mean values are controlled by the Lagrange multipliers.

The positivity and growth of the alignment with transverse momentum and centrality found in our model agree with general trends observed in the data; however, a satisfactory quantitative description of the data is not reproduced. This suggests that more realistic calculations of the spin polarization tensor should be used in the near future to analyze the data. This is also indicated by the dependence of our results on the parameter $\lambda$ — its growth from 1 to 3 improves the description of both the longitudinal polarization and alignment. This may be a signal for a deeper connection between these two effects that is worth pursuing.

The paper is organized as follows. In Section 2, we briefly review the thermal model with anisotropic transverse flow and introduce the projected thermal vorticity together with the scale parameter $\lambda$. Section 3 presents the theoretical framework for the spin alignment of vector mesons. Our numerical results for the $p_{\rm T}$-integrated alignment, its transverse momentum, centrality, and quantization-axis dependence are discussed in Section 4. Finally, Section 5 contains a summary and outlook.

*Notation and conventions*: For the Levi-Civita tensor $\epsilon^{\mu\nu\alpha\beta}$, we follow the convention $\epsilon^{0123} = -\epsilon_{0123} = +1$. The metric tensor is of the form $g_{\mu\nu} = \mathrm{diag}(+1, -1, -1, -1)$. We use boldface symbols to denote three vectors, and their scalar products are written as $\boldsymbol{a}\cdot\boldsymbol{b}$. The particles are always considered on the mass shell with the energy $E_{\boldsymbol{p}} = \sqrt{m^2 + \boldsymbol{p}^2}$. Throughout the text, we make use of natural units, $\hbar = c = k_{\rm B} = 1$.

## 2. Thermal model

We employ a thermal model based on the assumption of simultaneous kinetic and chemical freeze-out [76, 77]. In this single freeze-out approach, all hadrons decouple from the medium at the same proper time $\tau_{\rm f}$ and temperature $T_{\rm f}$. Despite its simplicity, this model has been remarkably successful in reproducing transverse-momentum spectra and elliptic flow coefficients across a range of centralities in heavy-ion collisions [71, 78].

In its standard formulation, the model is characterized by four parameters: the freeze-out temperature $T_{\rm f}$, the baryon chemical potential $\mu_B$, the proper time $\tau_{\rm f}$, and the maximum transverse size of the fireball $r_{\rm max}$. The temperature and the chemical potential are fixed by measuring hadronic yield ratios, while the system size and proper time are extracted from the fits to the transverse-momentum spectra. At the ultrarelativistic energies that we are considering here, the net baryon at midrapidity is negligible and we set $\mu_B = 0$.

Since the spin alignment is interconnected to longitudinal spin polarization, which in turn is connected to the anisotropy of collective flow, we make use of an extended version of the thermal model that includes azimuthal asymmetry in the transverse hydrodynamic flow. The four-velocity field is parameterized as

$$u^\mu = \frac{1}{N}\left(t,\, x\sqrt{1+\delta}\,,\, y\sqrt{1-\delta}\,, z\right), \tag{1}$$

where the parameter $N$ is determined from the normalization condition $u^\mu u_\mu = 1$

$$N = \sqrt{\tau_{\rm f}^2 - (x^2 - y^2)\,\delta}\,, \tag{2}$$

and $\tau_{\rm f}$ is the proper time at freeze-out

$$\tau_{\rm f}^2 = t^2 - \left(x^2 + y^2 + z^2\right)\,. \tag{3}$$

The parameter $\delta$ controls the anisotropy of the transverse flow (the elliptic flow). Together with $\delta$, the parameter $\epsilon$ is introduced that determines the asymmetry in the transverse space. Both $\delta$ and $\epsilon$ were previously fitted to the PHENIX data at $\sqrt{s_{NN}} = 130$ GeV for three centrality classes: 0–15%, 15–30%, and 30–60%, with the freeze-out temperature $T_{\rm f} = 0.165$ GeV [71, 78][1].

In our case, we also introduce additional assumptions related to the spin physics: first, we use projected thermal vorticity (the thermal vorticity tensor with all "electric"-like components neglected, *i.e.*, we set $\varpi_{0i} = 0$), second, we rescale the thermal vorticity by a factor $\lambda$, which controls the magnitude of the longitudinal polarization. We have found that the values $\lambda = 1$ and $\lambda = 3$ describe the longitudinal polarization of $\Lambda$ hyperons with $\chi^2$ (per one degree of freedom) below 2, see Fig. 1.

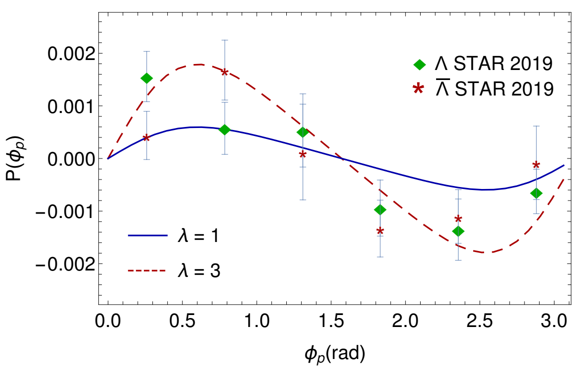


Fig. 1. Longitudinal spin polarization of $\Lambda$ hyperons compared to the experimental data [3]. The blue solid (red dashed) line shows the model result with projected thermal vorticity and $\lambda = 1$ ($\lambda = 3$).

[1] The parameters of the thermal model were fixed for the beam energy $\sqrt{s_{NN}} = 130$ GeV, while the polarization data analyzed here refer to $\sqrt{s_{NN}} = 200$ GeV. We neglect small differences in the thermal parameters for these two energies.

We note that the thermal model [71, 78] was not only used by us in previous studies of longitudinal polarization but also used in alignment analyses [54, 57], however, in different contexts (influence of second-order hydrodynamic gradients [54] and spin-vorticity non-equilibrium effects [57]).

## 3. Theoretical framework for spin alignment

The spin density matrix for spin-1 particles in the adjoint representation reads [70]

$$\rho^S_{rs*} = \frac{1}{3}\left(\delta_{rs} - \frac{3i}{2}P^k_* \epsilon_{krs} - \sqrt{6}\,T_{rs*}\right) , \tag{4}$$

where $P^k_*$ is the spin polarization vector and $T_{rs*}$ are the tensor polarizabilities, both defined in the particle rest frame (PRF) denoted by asterisk. Here, the spin densities $r, s$ range from 1 to 3. In local equilibrium, the spin density matrix takes the form

$$\rho^S_{\rm eq} = \frac{\exp[\boldsymbol{\alpha}\cdot\boldsymbol{S}]}{2\cosh\alpha + 1} , \tag{5}$$

where $\boldsymbol{\alpha} = -\boldsymbol{b}_*$, with $\boldsymbol{b}_*$ being the magnetic-like component of the spin polarization tensor $\omega_{\mu\nu}$ in PRF [23]

$$\boldsymbol{b}_* = \frac{1}{m}\left(E_{\boldsymbol{p}}\,\boldsymbol{b} - \boldsymbol{p}\times\boldsymbol{e} - \frac{\boldsymbol{p}\cdot\boldsymbol{b}}{E_{\boldsymbol{p}}+m}\boldsymbol{p}\right) . \tag{6}$$

The use of projected thermal vorticity means that we use the condition $\boldsymbol{e}=0$. The vector $\boldsymbol{S}$ represents three spin matrices in the adjoint representation, $(S^j)_{k\ell} = -i\epsilon_{jk\ell}$. The components of $\boldsymbol{b}$ read

$$b^1 = \frac{\lambda yz}{TN^3}\left(\sqrt{1-\delta} - 1 + \delta\right) , \tag{7}$$

$$b^2 = \frac{\lambda xz}{TN^3}\left(1 + \delta - \sqrt{1+\delta}\right) , \tag{8}$$

$$b^3 = -\frac{\lambda xy\sqrt{1-\delta^2}}{TN^3}\left(\sqrt{1+\delta} - \sqrt{1-\delta}\right) . \tag{9}$$

The alignment $A$ measured experimentally is defined by the central element $\rho_{00}$ of the spin density matrix in the representation where the spin matrix $J_y$ is diagonal [11]. Including the effect of a unitary transformation from this representation to the adjoint representation, we find [70]

$$A \equiv \rho_{00} - \frac{1}{3} = -\sqrt{\frac{2}{3}}T^*_{22} = -\frac{\left(3\hat{\alpha}_2^2 - 1\right)(\cosh\alpha - 1)}{3(2\cosh\alpha + 1)} , \tag{10}$$

where $\hat{\alpha}_2 = \alpha_2/|\boldsymbol{\alpha}|$ is the $y$-component of the unit vector along $\boldsymbol{\alpha}$. More generally, if the alignment measurement uses the $i^{\rm th}$ axis for spin quantization, then the definition of the alignment is

$$A_i = -\frac{\left(3\hat{\alpha}_i^2 - 1\right)(\cosh\alpha - 1)}{3(2\cosh\alpha + 1)}\,. \tag{11}$$

We note that $A_i$s satisfy the condition $A_1 + A_2 + A_3 = 0$ (which reflects the condition for having a traceless tensor $T^*_{rs}$). We also observe that for an isotropic spin system, we have $\hat{\alpha}_i^2 = 1/3\,(i = 1,2,3)$ that yields a vanishing alignment.

The momentum-dependent alignment is obtained by averaging over the freeze-out hypersurface $\Sigma_\mu$

$$A(p) = \frac{\displaystyle\int \mathrm{d}\Sigma_\mu\, p^\mu\, \mathcal{Z}\, f_0(x,p)\, A(x,p)}{\displaystyle\int \mathrm{d}\Sigma_\mu\, p^\mu\, \mathcal{Z}\, f_0(x,p)}\,, \tag{12}$$

where $f_0 = \exp[-p\cdot u/T_{\rm f}]$ is the Boltzmann distribution of particles (in our case, the $\phi$ and $K^{*0}$ mesons), and $\mathcal{Z} = 2\cosh\alpha + 1$, which is the normalization of spin density matrix.

## 4. Results

In this section, we present our numerical results for the parameter $\rho_{00}$ of $\phi$ and $K^{*0}$ mesons[2]. The model parameters used in the calculations are listed in Table 1. The masses of the mesons are: $m_\phi = 1.019$ GeV and $m_{K^{*0}} = 0.892$ GeV.

Table 1. Thermal model parameters used to describe the PHENIX data at $\sqrt{s_{NN}} = 130$ GeV, see Refs. [71, 78].

| Centrality [%] | $\epsilon$ | $\delta$ | $\tau_{\rm f}$ [fm] | $r_{\rm max}$ [fm] |
|---|---|---|---|---|
| 0–15 | 0.055 | 0.12 | 7.666 | 6.540 |
| 15–30 | 0.097 | 0.26 | 6.258 | 5.417 |
| 30–60 | 0.137 | 0.37 | 4.266 | 3.779 |

[2] To compare our results directly with the data, we show our results for $\rho_{00}$ rather than for $A$.

### *4.1. Transverse-momentum integrated alignment*

We begin by examining the $p_T$-integrated values of $\rho_{00}$ for the $\phi$ and $K^{*0}$ mesons. The integration ranges follow the STAR coverage: $1.2 \leq p_T \leq 5.4$ GeV for $\phi$ mesons and $1.0 \leq p_T \leq 5.0$ GeV for $K^{*0}$ mesons [11]. Figure 2 displays the $p_T$-integrated $\rho_{00}$ as a function of meson mass for 30–60% centrality class. Both $\phi$ and $K^{*0}$ mesons exhibit $\rho_{00} > 1/3$, indicating a positive spin alignment. The deviation from 1/3 is larger for the heavier $\phi$ meson compared to the lighter $K^{*0}$, showing a mass ordering of the alignment. Increasing $\lambda$ from 1 to 3 enhances the alignment but does not fully bridge the gap between the model predictions and the data.

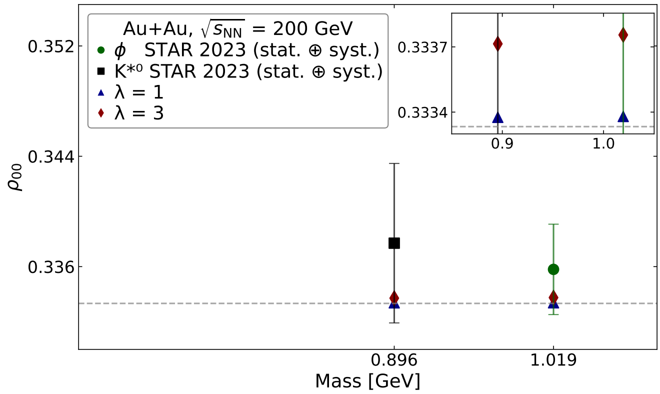


Fig. 2. Transverse-momentum integrated $\rho_{00}$ for $\phi$ and $K^{*0}$ mesons as a function of mass. Experimental data from STAR [11].

### *4.2. Transverse-momentum dependence*

Figures 3 and 4 show the $p_T$-differential $\rho_{00}$ for $\phi$ and $K^{*0}$ mesons, respectively, compared with the STAR data [11]. The corresponding numerical values are tabulated in Tables 2 and 3. For both species of mesons, the model predicts a monotonically increasing $\rho_{00}$ with $p_T$. The $\lambda = 3$ case produces deviations at the level of $10^{-3}$ (for the largest values of momenta).

### *4.3. Centrality dependence*

Figures 5 and 6 present the centrality dependence of $\rho_{00}$ for $\phi$ and $K^{*0}$ mesons, respectively. The corresponding numerical values are collected in Table 4. The model predicts an increase of $\rho_{00}$ from central to peripheral collisions, however, the centrality dependence observed in the experiment is much stronger.

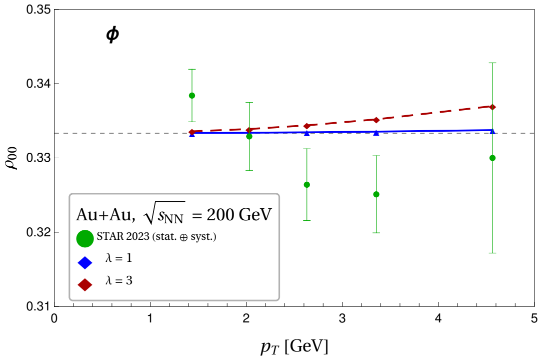


Fig. 3. Transverse-momentum dependence of $\rho_{00}$ for $\phi$ mesons. The solid blue and dashed red lines show our results for $\lambda = 1$ and 3, respectively. Experimental data from STAR [11].

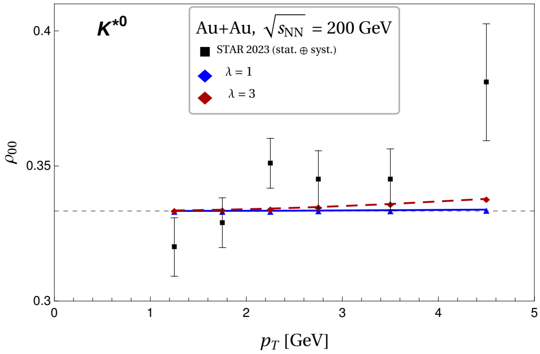


Fig. 4. The same as Fig. 3 but for $K^{*0}$ mesons.

Table 2. Theoretical values of $\rho_{00}$ for $\phi$ mesons with $\lambda = 1$ and $\lambda = 3$ compared to STAR measurements [11] with respect to the second-order event plane.

| $p_{\mathrm{T}}$ [GeV] | $\rho_{00}^{\mathrm{th}}$ $\lambda = 1$ | $\rho_{00}^{\mathrm{th}}$ $\lambda = 3$ | $\rho_{00}$ |
|---|---|---|---|
| 1.4339 | 0.333361 | 0.333581 | 0.3384 |
| 2.0306 | 0.333396 | 0.333897 | 0.3329 |
| 2.6304 | 0.333451 | 0.334388 | 0.3264 |
| 3.3535 | 0.333543 | 0.335199 | 0.3251 |
| 4.5640 | 0.333747 | 0.336982 | 0.3300 |

Table 3. The same as Table 2 but for $K^{*0}$ mesons.

| $p_T$ [GeV] | $\rho_{00}^{th}$ $\lambda = 1$ | $\rho_{00}^{th}$ $\lambda = 3$ | $\rho_{00}$ |
|---|---|---|---|
| 1.25 | 0.333356 | 0.333538 | 0.320 |
| 1.75 | 0.333386 | 0.333804 | 0.329 |
| 2.25 | 0.333433 | 0.334222 | 0.351 |
| 2.75 | 0.333498 | 0.334797 | 0.345 |
| 3.50 | 0.333626 | 0.335928 | 0.345 |
| 4.50 | 0.333845 | 0.337830 | 0.381 |

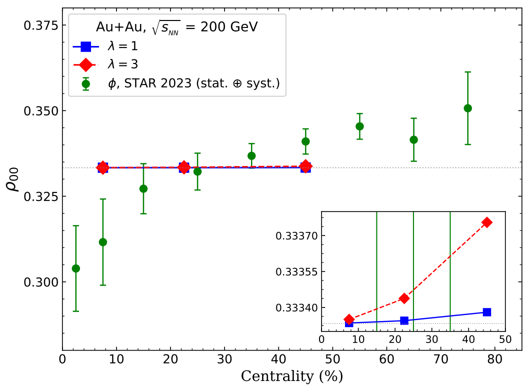


Fig. 5. Centrality dependence of $\rho_{00}$ for $\phi$ mesons. The solid blue and dashed red lines show model results for $\lambda = 1$ and 3, respectively. Experimental data are from STAR [11].

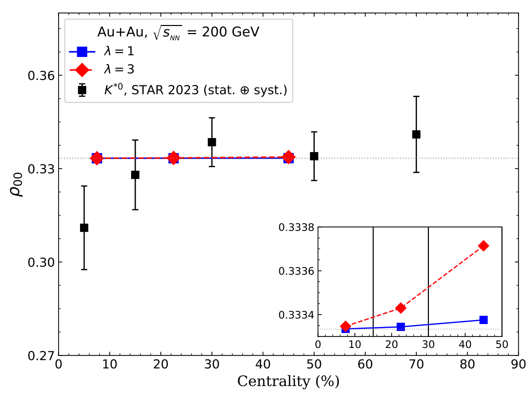


Fig. 6. The same as Fig. 5 but for $K^{*0}$ mesons.

Table 4. Centrality dependence of theoretical $\rho_{00}$ for $\phi$ and $K^{*0}$ mesons with $\lambda = 1$ and $\lambda = 3$ in Au+Au collisions at $\sqrt{s_{NN}} = 200$ GeV.

| Centrality [%] | Meson | $\rho_{00}^{\mathrm{th}}$ | |
|---|---|---|---|
| | | $\lambda = 1$ | $\lambda = 3$ |
| 0–15 | $\phi$ | 0.333335 | 0.333350 |
| 15–30 | $\phi$ | 0.333345 | 0.333438 |
| 30–60 | $\phi$ | 0.333380 | 0.333755 |
| 0–15 | $K^{*0}$ | 0.333335 | 0.333347 |
| 15–30 | $K^{*0}$ | 0.333344 | 0.333430 |
| 30–60 | $K^{*0}$ | 0.333376 | 0.333714 |

### *4.4. Quantization-axis dependence*

We have also calculated the alignment assuming spin quantization along the $x$-axis. In this case, one has to calculate the alignment $A_1$, see Eq. (11). Our calculations of $A_1$ give again positive alignment, which does not agree with the experimental result that shows that $A_1$ is negative.

## 5. Summary

We have performed the analysis of spin alignment of $\phi$ and $K^{*0}$ vector mesons within a thermal model for heavy-ion collisions at the top RHIC energies. A common spin local equilibrium was assumed for $\Lambda$ hyperons and vector mesons. Our main findings can be summarized as follows:

1. The model predicts, in contrast to many other physical analyzes [17, 19, 26, 40, 55], a positive alignment and monotonic increase of $\rho_{00}$ with transverse momentum and centrality.
2. The mass ordering is observed, with the heavier $\phi$ meson exhibiting a slightly larger deviation of $\rho_{00}$ from 1/3 compared to $K^{*0}$.
3. Quantitatively, the model with $\lambda = 1$ produces deviations $\rho_{00} - 1/3$ at the $10^{-4}$ level, which are below the experimental values. Increasing $\lambda$ to 3 enhances the deviations to the $10^{-3}$ level (for the largest considered values of transverse momentum), improving the alignment, but still cannot explain quantitatively the data.

The fact that changes in the scale parameter $\lambda$ simultaneously affect the magnitude of the longitudinal polarization of $\Lambda$ and the spin alignment of the vector mesons suggests that there is a correlation between these two observables that deserves a more detailed study in the future.

Soham Banerjee and A.J. gratefully acknowledge the Department of Atomic Energy (DAE), India, for financial support. Samapan Bhadury acknowledges support from the Anusandhan National Research Foundation (ANRF), India, through National Postdoctoral Fellowship, File No. PDF/2025/004233. W.F. and R.R. were supported in part by the National Science Centre (NCN), Poland, grant No. 2022/47/B/ST2/01372. Samapan Bhadury, W.F., and R.R. would like to acknowledge the kind hospitality of the National Institute of Science Education and Research (NISER), Jatni, India, where this analysis was initiated.

## REFERENCES

[1] STAR Collaboration (L. Adamczyk *et al.*), «Global $\Lambda$ hyperon polarization in nuclear collisions», *Nature* **548**, 62 (2017).

[2] STAR Collaboration (J. Adam *et al.*), «Global polarization of $\Lambda$ hyperons in Au+Au collisions at $\sqrt{s_{NN}} = 200$ GeV», *Phys. Rev. C* **98**, 014910 (2018).

[3] STAR Collaboration (J. Adam *et al.*), «Polarization of $\Lambda(\bar{\Lambda})$ Hyperons along the Beam Direction in Au+Au Collisions at $\sqrt{s_{NN}} = 200$ GeV», *Phys. Rev. Lett.* **123**, 132301 (2019).

[4] ALICE Collaboration (S. Acharya *et al.*), «Global polarization of $\Lambda$ and $\bar{\Lambda}$ hyperons in Pb–Pb collisions at 2.76 and 5.02 TeV», *Phys. Rev. C* **101**, 044611 (2020); *Erratum ibid.* **105**, 029902 (2022).

[5] STAR Collaboration (J. Adam *et al.*), «Global Polarization of $\Xi$ and $\Omega$ Hyperons in Au+Au Collisions at $\sqrt{s_{NN}} = 200$ GeV», *Phys. Rev. Lett.* **126**, 162301 (2021); *Erratum ibid.* **131**, 089901 (2023).

[6] ALICE Collaboration (S. Acharya *et al.*), «Polarization of $\Lambda$ and $\bar{\Lambda}$ Hyperons along the Beam Direction in Pb–Pb Collisions at $\sqrt{s_{NN}} = 5.02$ TeV», *Phys. Rev. Lett.* **128**, 172005 (2022).

[7] STAR Collaboration (M.S. Abdallah *et al.*), «Global $\Lambda$-hyperon polarization in Au+Au collisions at $\sqrt{s_{NN}} = 3$ GeV», *Phys. Rev. C* **104**, L061901 (2021).

[8] HADES Collaboration (R. Abou Yassine *et al.*), «Measurement of global polarization of $\Lambda$ hyperons in few-GeV heavy-ion collisions», *Phys. Lett. B* **835**, 137506 (2022).

[9] STAR Collaboration (M.I. Abdulhamid *et al.*), «Global polarization of $\Lambda$ and $\bar{\Lambda}$ hyperons in Au+Au collisions at $\sqrt{s_{NN}} = 19.6$ and 27 GeV», *Phys. Rev. C* **108**, 014910 (2023).

[10] ALICE Collaboration (S. Acharya *et al.*), «Evidence of Spin-Orbital Angular Momentum Interactions in Relativistic Heavy-Ion Collisions», *Phys. Rev. Lett.* **125**, 012301 (2020).

[11] STAR Collaboration (M.S. Abdallah *et al.*), «Pattern of global spin alignment of $\phi$ and $K^{*0}$ mesons in heavy-ion collisions», *Nature* **614**, 244 (2023).

[12] ALICE Collaboration (S. Acharya *et al.*), «Measurement of the $J/\psi$ Polarization with Respect to the Event Plane in Pb–Pb Collisions at the LHC», *Phys. Rev. Lett.* **131**, 042303 (2023).

[13] F. Becattini *et al.*, «Spin polarization in relativistic heavy-ion collisions», *Int. J. Mod. Phys. E* **33**, 2430006 (2024).

[14] T. Niida, S.A. Voloshin, «Polarization phenomenon in heavy-ion collisions», *Int. J. Mod. Phys. E* **33**, 2430010 (2024).

[15] J.-H. Chen *et al.*, «Vector meson's spin alignments in high energy reactions», *Sci. China Phys. Mech. Astron.* **68**, 211001 (2025).

[16] Z.-T. Liang, X.-N. Wang, «Globally Polarized Quark–Gluon Plasma in Noncentral $A+A$ Collisions», *Phys. Rev. Lett.* **94**, 102301 (2005); *Erratum ibid.* **96**, 039901 (2006).

[17] Z.-T. Liang, X.-N. Wang, «Spin alignment of vector mesons in non-central $A+A$ collisions», *Phys. Lett. B* **629**, 20 (2005).

[18] F. Becattini, L. Tinti, «The ideal relativistic rotating gas as a perfect fluid with spin», *Ann. Phys.* **325**, 1566 (2010).

[19] Y.-G. Yang, R.-H. Fang, Q. Wang, X.-N. Wang, «Quark coalescence model for polarized vector mesons and baryons», *Phys. Rev. C* **97**, 034917 (2018).

[20] D. Montenegro, L. Tinti, G. Torrieri, «Ideal relativistic fluid limit for a medium with polarization», *Phys. Rev. D* **96**, 056012 (2017); *Addendum ibid.* **96**, 079901 (2017).

[21] D. Montenegro, L. Tinti, G. Torrieri, «Sound waves and vortices in a polarized relativistic fluid», *Phys. Rev. D* **96**, 076016 (2017).

[22] W. Florkowski, B. Friman, A. Jaiswal, E. Speranza, «Relativistic fluid dynamics with spin», *Phys. Rev. C* **97**, 041901 (2018).

[23] W. Florkowski *et al.*, «Spin-dependent distribution functions for relativistic hydrodynamics of spin-$\frac{1}{2}$ particles», *Phys. Rev. D* **97**, 116017 (2018).

[24] W. Florkowski, A. Kumar, R. Ryblewski, «Thermodynamic *versus* kinetic approach to polarization-vorticity coupling», *Phys. Rev. C* **98**, 044906 (2018).

[25] Y. Sun, C.M. Ko, «Azimuthal angle dependence of the longitudinal spin polarization in relativistic heavy ion collisions», *Phys. Rev. C* **99**, 011903 (2019).

[26] X.-L. Sheng, L. Oliva, Q. Wang, «What can we learn from the global spin alignment of mesons in heavy-ion collisions?», *Phys. Rev. D* **101**, 096005 (2020); *Erratum ibid.* **105**, 099903 (2022).

[27] K. Hattori *et al.*, «Fate of spin polarization in a relativistic fluid: An entropy-current analysis», *Phys. Lett. B* **795**, 100 (2019).

[28] Y. Xie, D. Wang, L.P. Csernai, «Fluid dynamics study of the $\Lambda$ polarization for Au+Au collisions at $\sqrt{s_{NN}} = 200$ GeV», *Eur. Phys. J. C* **80**, 39 (2020).

[29] W. Florkowski, A. Kumar, R. Ryblewski, R. Singh, «Spin polarization evolution in a boost-invariant hydrodynamical background», *Phys. Rev. C* **99**, 044910 (2019).

[30] N. Weickgenannt *et al.*, «Kinetic theory for massive spin-$\frac{1}{2}$ particles from the Wigner-function formalism», *Phys. Rev. D* **100**, 056018 (2019).

[31] N. Weickgenannt *et al.*, «Generating Spin Polarization from Vorticity through Nonlocal Collisions», *Phys. Rev. Lett.* **127**, 052301 (2021).

[32] S. Bhadury *et al.*, «Dissipative spin dynamics in relativistic matter», *Phys. Rev. D* **103**, 014030 (2021).

[33] S. Shi, C. Gale, S. Jeon, «From chiral kinetic theory to relativistic viscous spin hydrodynamics», *Phys. Rev. C* **103**, 044906 (2021).

[34] R. Singh, G. Sophys, R. Ryblewski, «Spin polarization dynamics in the Gubser-expanding background», *Phys. Rev. D* **103**, 074024 (2021).

[35] C. Yi, S. Pu, D.-L. Yang, «Reexamination of local spin polarization beyond global equilibrium in relativistic heavy ion collisions», *Phys. Rev. C* **104**, 064901 (2021).

[36] D.-L. Wang, S. Fang, S. Pu, «Analytic solutions of relativistic dissipative spin hydrodynamics with Bjorken expansion», *Phys. Rev. D* **104**, 114043 (2021).

[37] M. Hongo *et al.*, «Relativistic spin hydrodynamics with torsion and linear response theory for spin relaxation», *J. High Energy Phys.* **2021**, 150 (2021).

[38] W. Florkowski, R. Ryblewski, R. Singh, G. Sophys, «Spin polarization dynamics in the non-boost-invariant background», *Phys. Rev. D* **105**, 054007 (2022).

[39] D.-L. Wang, X.-Q. Xie, S. Fang, S. Pu, «Analytic solutions of relativistic dissipative spin hydrodynamics with radial expansion in Gubser flow», *Phys. Rev. D* **105**, 114050 (2022).

[40] X.-L. Sheng *et al.*, «Spin Alignment of Vector Mesons in Heavy-Ion Collisions», *Phys. Rev. Lett.* **131**, 042304 (2023).

[41] X.-L. Sheng *et al.*, «Relativistic spin dynamics for vector mesons», *Phys. Rev. D* **109**, 036004 (2024).

[42] M. Hongo *et al.*, «Spin relaxation rate for heavy quarks in weakly coupled QCD plasma», *J. High Energy Phys.* **2022**, 263 (2022).

[43] N. Weickgenannt, D. Wagner, E. Speranza, D. H. Rischke, «Relativistic second-order dissipative spin hydrodynamics from the method of moments», *Phys. Rev. D* **106**, 096014 (2022).

[44] G. Sarwar *et al.*, «Causality and stability of relativistic spin hydrodynamics», *Phys. Rev. D* **107**, 054031 (2023).

[45] D. Wagner, N. Weickgenannt, D.H. Rischke, «Lorentz-covariant nonlocal collision term for spin-$\frac{1}{2}$ particles», *Phys. Rev. D* **106**, 116021 (2022).

[46] D. Wagner, N. Weickgenannt, E. Speranza, «Generating tensor polarization from shear stress», *Phys. Rev. Res.* **5**, 013187 (2023).

[47] A. Kumar, B. Müller, D.-L. Yang, «Spin polarization and correlation of quarks from the glasma», *Phys. Rev. D* **107**, 076025 (2023).

[48] R. Biswas *et al.*, «Relativistic second-order spin hydrodynamics: An entropy-current analysis», *Phys. Rev. D* **108**, 014024 (2023).

[49] N. Weickgenannt, «Linearly stable and causal relativistic first-order spin hydrodynamics», *Phys. Rev. D* **108**, 076011 (2023).

[50] M. Kiamari, N. Sadooghi, M.S. Jafari, «Relativistic magnetohydrodynamics of a spinful and vortical fluid: Entropy current analysis», *Phys. Rev. D* **109**, 036024 (2024).

[51] S. Fang, S. Pu, D.-L. Yang, «Spin polarization and spin alignment from quantum kinetic theory with self-energy corrections», *Phys. Rev. D* **109**, 034034 (2024).

[52] A. Palermo, F. Becattini, «Exact spin polarization of massive and massless particles in relativistic fluids at global equilibrium», *Eur. Phys. J. Plus* **138**, 547 (2023).

[53] A. Palermo, «Exact polarization of particles of any spin at global equilibrium», *EPJ Web Conf.* **296**, 04008 (2024).

[54] A. Kumar, D.-L. Yang, P. Gubler, «Spin alignment of vector mesons by second-order hydrodynamic gradients», *Phys. Rev. D* **109**, 054038 (2024).

[55] A. Kumar, B. Müller, D.-L. Yang, «Spin alignment of vector mesons by glasma fields», *Phys. Rev. D* **108**, 016020 (2023).

[56] J. Chen, Z.-T. Liang, Y.-G. Ma, Q. Wang, «Global spin alignment of vector mesons and strong force fields in heavy-ion collisions», *Sci. Bull.* **68**, 874 (2023).

[57] K.J. Gonçalves, G. Torrieri, R. Ryblewski, «Meson spin alignment and baryon polarization from coalescence with spin-vorticity nonequilibrium», *Phys. Rev. C* **112**, 014901 (2025).

[58] E. Grossi, A. Palermo, I. Zahed, «Polarized $\phi$ meson rates with viscous corrections at energies available at the BNL Relativistic Heavy Ion Collider», *Phys. Rev. C* **111**, 014914 (2025).

[59] F. Sun *et al.*, «Chiral phase transition and spin alignment of vector mesons in the polarized-Polyakov-loop Nambu–Jona-Lasinio model under rotation», *Phys. Rev. D* **109**, 116017 (2024).

[60] E. Grossi, A. Palermo, I. Zahed, «Polarization of the $\phi$ meson in the hadronic phase with nucleon scatterings and a viscous hydrodynamic background», *Phys. Rev. C* **112**, 064910 (2025).

[61] A. Arslan *et al.*, «In-plane transverse polarization in heavy-ion collisions», *Phys. Rev. C* **113**, 034920 (2026), `arXiv:2509.00796 [nucl-th]`.

[62] F. Becattini, I. Karpenko, «Collective Longitudinal Polarization in Relativistic Heavy-Ion Collisions at Very High Energy», *Phys. Rev. Lett.* **120**, 012302 (2018).

[63] S.Y.F. Liu, Y. Yin, «Spin polarization induced by the hydrodynamic gradients», *J. High Energy Phys.* **2021**, 188 (2021).

[64] B. Fu *et al.*, «Shear-Induced Spin Polarization in Heavy-Ion Collisions», *Phys. Rev. Lett.* **127**, 142301 (2021).

[65] F. Becattini, M. Buzzegoli, A. Palermo, «Spin-thermal shear coupling in a relativistic fluid», *Phys. Lett. B* **820**, 136519 (2021).

[66] F. Becattini *et al.*, «Local Polarization and Isothermal Local Equilibrium in Relativistic Heavy Ion Collisions», *Phys. Rev. Lett.* **127**, 272302 (2021).

[67] S.K. Singh, R. Ryblewski, W. Florkowski, «Spin dynamics with realistic hydrodynamic background for relativistic heavy-ion collisions», *Phys. Rev. C* **111**, 024907 (2025).

[68] Sapna, S.K. Singh, D. Wagner, «Spin polarization of $\Lambda$ hyperons from dissipative spin hydrodynamics», *Phys. Rev. C* **112**, 054902 (2025).

[69] Z. Liu, Z. Li, W. Zha, Z. Tang, «Energy dependence of rescattering effect on vector mesons spin alignment at RHIC», *Phys. Lett. B* **873**, 140161 (2026).

[70] W. Florkowski, S.K. Kar, V. Mykhaylova, «Spin alignment, tensor polarizabilities, and local equilibrium for spin-1 particles», *Acta Phys. Pol. B* **57**, 6-A4 (2026), `arXiv:2602.00819 [nucl-th]`.

[71] W. Broniowski, A. Baran, W. Florkowski, «Thermal model for RHIC, part II: elliptic flow and HBT radii», *AIP Conf. Proc.* **660**, 185 (2003).

[72] W. Florkowski, A. Kumar, R. Ryblewski, A. Mazeliauskas, «Longitudinal spin polarization in a thermal model», *Phys. Rev. C* **100**, 054907 (2019).

[73] W. Florkowski, A. Kumar, A. Mazeliauskas, R. Ryblewski, «Effect of thermal shear on longitudinal spin polarization in a thermal model», *Phys. Rev. C* **105**, 064901 (2022).

[74] S. Banerjee *et al.*, «Longitudinal spin polarization in a thermal model with dissipative corrections», *Phys. Rev. C* **111**, 064912 (2025).

[75] S.A. Voloshin, «Vorticity and particle polarization in heavy ion collisions (experimental perspective)», *EPJ Web Conf.* **171**, 07002 (2018).

[76] W. Broniowski, W. Florkowski, «Description of the RHIC $p_\perp$ Spectra in a Thermal Model with Expansion», *Phys. Rev. Lett.* **87**, 272302 (2001).

[77] W. Florkowski, W. Broniowski, M. Michalec, «Thermal Analysis of Particle Ratios and $p_\perp$ Spectra at RHIC», *Acta Phys. Pol. B* **33**, 761 (2002).

[78] A. Baran, Ph.D. Thesis, Institute of Nuclear Physics, Kraków, Poland, 2004.